Electronic structure of the two-dimensionally ordered Mn/Cu(110) magnetic surface alloy

U. Manju,[1,2,*] D. Topwal,[3] G. Rossi,[2,4] and I. Vobornik[2]
[1]*International Centre for Theoretical Physics, Strada Costiera 11, 34100 Trieste, Italy*
[2]*TASC Laboratory, IOM-CNR, SS 14, km 163.5, I-34149 Trieste, Italy*
[3]*Sincrotrone Trieste, SS 14, km 163.5, I-34149 Trieste, Italy*
[4]*Università di Modena e Reggio Emilia, via Campi 213/A, I-41100 Modena, Italy*
(Received 4 March 2010; revised manuscript received 26 May 2010; published 29 July 2010)

We report a systematic investigation of the electronic properties and correlation effects in a two-dimensional magnetic surface alloy Mn/Cu(110) using a combination of spectroscopic techniques ranging from the angle-resolved photoemission, x-ray photoelectron, and x-ray absorption spectroscopy. Our results show that increasing Mn concentration surprisingly induces a progressive charge redistribution on the Cu(110) substrate, increasing the electron occupancy of the Cu Shockley surface state. Furthermore, new Mn-induced surface bands are identified at the $\bar{X}$ symmetry point that are backfolded with respect to the Brillouin-zone boundary and expose a band gap in the occupied states. Distinct satellite features in both the core-level photoemission and absorption spectra for a wide range of Mn concentrations suggest the presence of strong electronic correlations and increased ordering of this alloy with respect to its other known counterparts, such as Mn/Cu(100) and Mn/Ni(110).

DOI: 10.1103/PhysRevB.82.035442 PACS number(s): 79.60.Dp, 73.20.At, 73.20.Hb

I. INTRODUCTION

Magnetically stabilized ordered surface alloys have attracted increasing attention due to the possibility of tailoring their properties for potential applications in data storage and spin-injection devices.[1,2] Materials pertaining to this class consist of a nonmagnetic metallic surface where the atoms with a magnetic moment arrange in superstructures. *Ab initio* electronic-structure calculations show that the stability of these surface alloys arises from the presence of a large magnetic moment of the constituent atoms. Mn and related compounds are of particular interest in this regard due to the high magnetic moment ($5\mu_B$) expected for Mn from Hund's rules. For instance, in the $c(2\times2)$ Mn/Cu(100) and $c(2\times2)$ Mn/Ni(100) surface alloys Mn magnetic moment reaches $3.75\mu_B$ and $3.5\mu_B$, respectively.[3–5] Mn-Cu surface alloys deserve special consideration as they get stabilized over wide temperature ranges and are characterized by a considerable atomic corrugation in the ordered surface layer while no ordered bulk Mn-Cu alloys exist.[3,6,7] The stability of these two-dimensional (2D) systems is due to the large gain in the magnetic energy associated with an outward buckling of the Mn atoms.[3,6,7]

Generally the electronic and magnetic properties of low dimensional systems, such as ultrathin films and surface alloys, are expected to be significantly different from their bulk counterparts. This is mainly because of a lower atomic coordination number and chemical environment on the surface as compared to the bulk. A reduced overlap of the electronic wave functions leads to the reduction in the electronic bandwidths and gives rise to an enhancement of the exchange splitting and the magnetic moments in ultrathin magnetic films.[8,9] The band width lowering also increases electronic localization and hence the correlations effects become increasingly important. In spite of such expectations, correlation effects have been addressed only in a few studies of magnetic surface alloys.[5,10]

The magnetically stabilized alloys have been investigated so far mostly on (100) surfaces, with a few exceptions which dealt with (110) surfaces.[11,12] Formation of a 2D, ordered $c(2\times2)$ Mn/Cu(110) surface alloy was studied from the structural and magnetic point of view and it was found that the Mn atoms buckle outward and the Cu atoms inward with a total buckling amplitude of 0.22 Å [17.2% of the ideal interlayer distance in Cu(110)].[11] It was further suggested that the buckling reverts the coupling between the Mn magnetic moments from antiparallel to parallel resulting in a long-range ferromagnetic order. A large Mn magnetic moment of $3.82\mu_B$ was predicted and proposed to be the origin of the large electronic-structure modifications that lead to the work-function change.[11]

Here we report a systematic investigation of the electronic properties and correlation effects in Mn/Cu(110) surface alloy with varying Mn concentrations. Using a combination of various spectroscopic techniques, ranging from the angle-resolved photoemission spectroscopy (ARPES), x-ray photoelectron spectroscopy (XPS), and x-ray absorption spectroscopy (XAS), we find that increasing Mn concentrations induce a progressive charge redistribution on the Cu(110) surface, resulting in an increase in the number of electrons occupying the Cu surface state (SS). The distinct satellite features are observed in both the XPS and XAS spectra for a wide range of Mn coverages, suggesting the presence of strong electronic correlations and an increased stability of this alloy with respect to its counterparts on Cu(100) or Ni(110).

II. EXPERIMENTAL DETAILS

A clean Cu(110) surface was prepared by repeated cycles of Ar^+-ion sputtering and annealing to 750 K. The clean surface has a sharp $p(1\times1)$ low-energy electron-diffraction (LEED) pattern while no C 1*s* and O 2*p* signals are present in the XPS spectra. Manganese was deposited *in situ*, using

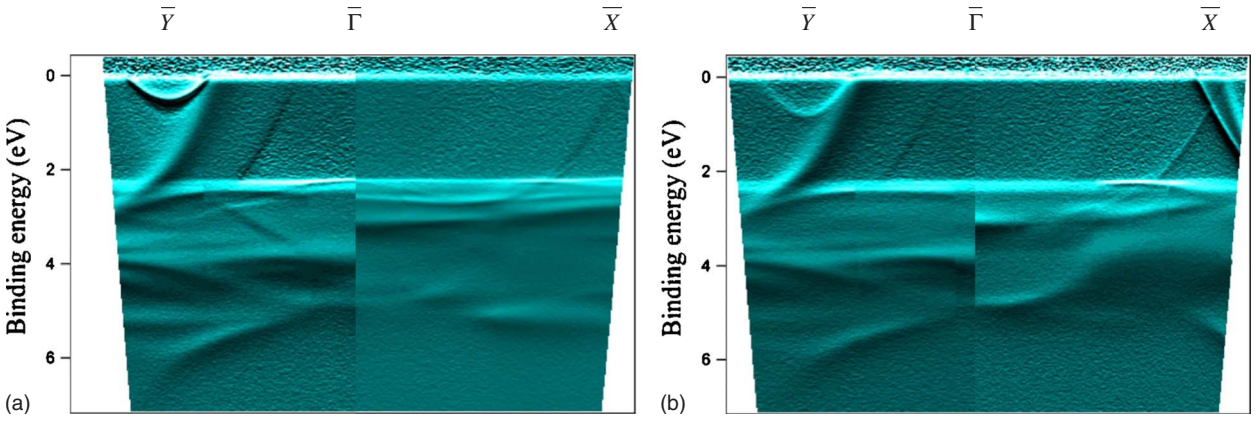

FIG. 1. (Color online) Band dispersions along the high-symmetry directions $\bar{\Gamma}$-$\bar{X}$ and $\bar{\Gamma}$-$\bar{Y}$ of the surface Brillouin zone for (a) clean Cu(110) and (b) 0.5 ML $c(2\times2)$ Mn/Cu(110) collected at 35 eV; note that an apparent mismatch at $\bar{\Gamma}$ between the features along $\bar{\Gamma}$-$\bar{X}$ and $\bar{\Gamma}$-$\bar{Y}$ is due to the matrix element effects and the consequent intensity reduction/enhancement as the experimental geometry changes for the two high-symmetry directions.

an electron-beam evaporation source, on the substrate kept at room temperature. The deposition rate was calibrated using a quartz thickness monitor. The pressure during the evaporation never exceeded 2×10^{-10} mbar. After Mn deposition, two different superstructures were observed by LEED: the submonolayer coverages lead to the formation of a $c(2\times2)$ superstructure characterized initially by faint and very diffused spots which become sharper and more intense with increasing coverage until a maximum order is reached at ~0.5 monolayer (ML). Beyond 0.5 ML Mn, $c(2\times2)$ spots get broader and decrease in intensity and vanish between 1.0 and 1.5 ML Mn. In this range, both $c(2\times2)$ and a higher (16×1) superstructure phase coexist. Beyond 2 ML, pure (16×1) phase remains. Our growth pattern follows the structure and growth phase diagram reported by Ross *et al.*[11] The presence of the representative LEED patterns and the absence of C 1*s* and O 2*p* signals in the photoemission spectra were verified for each sample preparation. All spectroscopic measurements were performed at the APE-INFM beamline at the Elettra synchrotron light source, Italy.[13] The two branch lines of APE, connected through a common sample preparation chamber, provide an ideal situation where one may study the electronic band dispersion as well as the core-level and absorption spectra on the very same sample surfaces. All ARPES measurements were performed using a linearly polarized light oriented in the storage ring plane and coplanar with the sample surface normal and the entrance slit of the electron energy analyzer (Scienta SES2002). For XPS measurements, an Omicron EA125 hemispherical electron energy analyzer was used. Mn $L_{2,3}$ XAS spectra were recorded by the total electron yield method. The base pressure in the experimental chambers was $<3\times10^{-11}$ mbar and data were collected at room temperature.

III. RESULTS AND DISCUSSION

We followed the band dispersions along the two high-symmetry directions ($\bar{\Gamma}$-$\bar{X}$ and $\bar{\Gamma}$-$\bar{Y}$) of the 2D surface Brillouin zone (SBZ) for clean Cu(110) [Fig. 1(a)] and for 0.5 ML $c(2\times2)$ Mn/Cu(110) [Fig. 1(b)]. In order to enhance the features near the Fermi energy (E_F) a first differential of intensities of measured band dispersions is shown. The position of E_F was estimated by measuring a polycrystalline Au sample in thermal and electrical contact with the Cu crystal. A comparison of the band structures shows that the Cu 3*d* and Mn 3*d* bands observed between 2 and 4.5 eV binding energies overlap for almost the entire SBZ making the gross electronic structures similar. However, already in this overall figure it is evident that surface alloying induces important modifications near the $\bar{X}$ and $\bar{Y}$ symmetry points.

Figure 2 shows a set of data collected at the $\bar{Y}$ symmetry point for clean Cu(110) and the alloys with increasing Mn content (0.125–0.5 ML). In Fig. 2(a), the well-known Shockley SS band of clean Cu(110) is observed, with a binding-energy minimum at ~0.49 eV, as reported previously.[14] With Mn deposition, the binding-energy minimum is shifting systematically toward higher binding energies [Figs. 2(b)–2(f)] while the diameter of the SS Fermi contour increases. The percentage gain in the area enclosed by the Fermi contour on going from clean Cu(110) to 0.5 ML $c(2\times2)$ Mn/Cu(110) is ~74% suggesting a significant increase in the number of charge carriers in the SS. It is well known that the presence of adsorbates modifies the electronic structure of surfaces. Different mechanisms contribute to the modification of the surface states, such as Pauli repulsion,[15,16] mixing and hybridization of electronic states,[17–19] charge transfer,[20,21] and polarization.[22,23] In the case of Mn/Cu(110), a direct charge transfer from Mn to Cu would have manifestations (shift in binding-energy positions/appearance of additional peaks) in the Mn 2*p* [discussed later in Fig. 4(a)] and Cu 2*p* core-level spectra (data not shown) which we do not observe. Hence we speculate the possibility of a Mn-induced charge redistribution in the Cu surface layer. As discussed previously, the structural investigations show that the Mn atoms induce a strong surface corrugation with inward/outward Cu/Mn relaxation with a total buckling amplitude of 0.22 Å [17.2% of the ideal interlayer distance

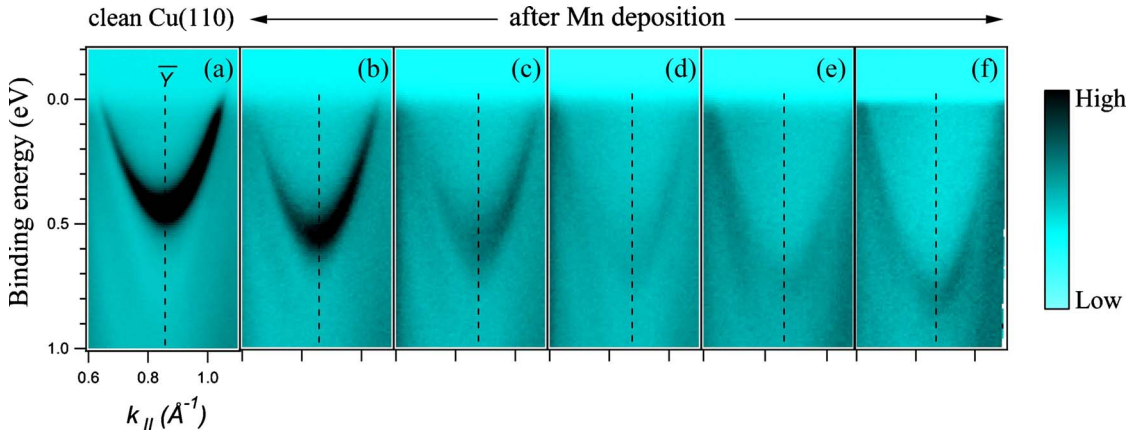

FIG. 2. (Color online) Shockley surface state around the $\bar{Y}$ symmetry point of the surface Brillouin zone for (a) clean Cu(110) and its evolution with increasing Mn concentration (b)–(f). The position of $\bar{Y}$ symmetry point is indicated by black dashed lines.

in Cu(110)].[11] Surface relaxation has already been pinpointed as a source of the local charge redistribution in Be(0001).[24,25] In the case of Mn/Cu(110), the corrugation might cause a local Cu charge transfer from the bulklike to the surface states.

Besides the increase in the SS Fermi contour, we also note the apparent change in the left-right asymmetry (with respect to $\bar{Y}$) of the SS intensity with increasing Mn coverage. In the recent work by Mulazzi *et al.*,[26] it was found that such photoemission intensity variation for *sp*-based Cu(111) surface state is directly linked to a change in the weight of the *d*-like final states available for the SS emission. In our case, it may imply that the *p* component of the *sp* originating Cu(110) surface state (which is linked to the transitions to *d* final states) changes due to hybridization with other symmetry components that "spill in" new charge in the SS. Quantitative understanding of the Mn-induced charge redistribution and of the associated photoemission intensity redistribution would require further theoretical calculations. It would be particularly challenging to understand the involvement of the above-mentioned phenomena in the large work-function change and hence the magnetism of the system.

Another impact of the Mn deposition on the electronic band structure are new bands formed around the $\bar{X}$ symmetry point of the Cu(110) SBZ as shown in Fig. 3. Experiments were performed by varying photon energies between 20 and 90 eV so as to optimize the cross-section ratio between the Mn- and Cu-induced bands. The set of data shown in Fig. 3 was collected using 46 eV, where the intensity of the Cu bulk bands is almost completely suppressed as shown in Fig. 3(a). Figure 3(b) shows the additional bands near the $\bar{X}$ symmetry point that appear at the coverage as low as 0.125 ML. Photon-energy-dependent measurements confirmed these bands to be of 2D character arising from surface alloying. For increasing Mn concentration, the bands gain in sharpness and intensity while remaining at the same k point and same binding energies in all the cases [Figs. 3(c)–3(e)]. Figure 3(f) shows that the bands are missing for 2.5 ML deposition where the (16×1) superstructure sets in. Therefore, these bands are pertinent to the $c(2\times2)$ superstructure uniquely. The results of Fig. 3 demonstrate that the Mn atoms start ordering into the $c(2\times2)$ structure even for very small Mn concentrations and that the overall local geometry and local interactions are not changing if some $c(2\times2)$ sites are left empty. Such Mn-derived bands around the $\bar{X}$ point have been reported previously in the band structures of single-layer MnN/MnCu/Cu(001) and 1 ML Mn/Cu(001). Similar to our case, the authors link their origin to the formation of an

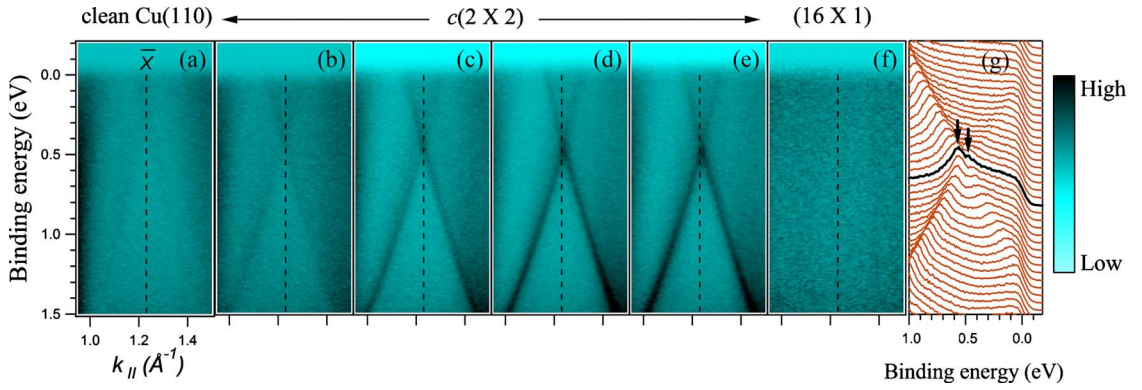

FIG. 3. (Color online) New electronic bands around the $\bar{X}$ symmetry point of the surface Brillouin zone for various Mn depositions: (a) clean Cu(110); (b)–(e) 0.125–0.5 ML Mn with $c(2\times2)$ arrangement; (f) 2.5 ML Mn coverage with (16×1) superstructure. (g): an expanded view of the EDCs for 0.5 ML $c(2\times2)$ Mn/Cu(110) near the $\bar{X}$ point indicating a possible band gap of $\sim$100 meV.

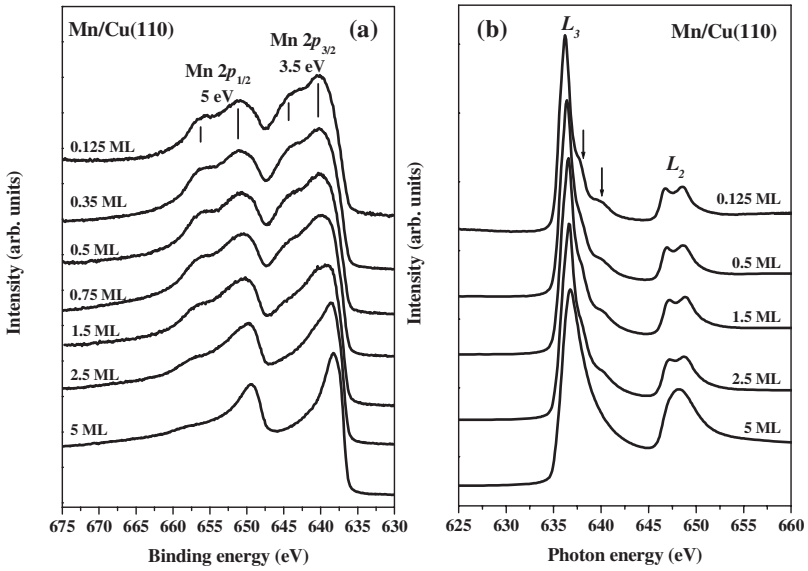

FIG. 4. (a) Mn $2p$ core-level photoemission spectra and (b) Mn $L_{2,3}$ x-ray absorption spectra for 0.125–5 ML Mn/Cu(110).

ordered single $c(2\times2)$ Mn/Cu(100) alloy layer at the interface.[1,27]

An expanded view of the energy distribution curves for 0.5 ML $c(2\times2)$ Mn/Cu(110) near the $\bar{X}$ point is shown in Fig. 3(g). One may clearly see from the figure that these new Mn-induced surface bands are backfolded with respect to $\bar{X}$, exposing a gap in the occupied states (at ~0.5 eV below E_F). Typically, introducing a (new) periodic potential leads to the band-gap opening at the (new) Brillouin-zone boundary. We remind here, however that $\bar{X}$ is the symmetry point of the Cu(110) substrate and not of the $c(2\times2)$ reconstruction and therefore this reasoning cannot be applied to our case. Similar band-gap opening has been reported in the electronic structure of Pb-Cu alloys where a considerable buckling of ~0.2 Å in the Pb layer and an even larger, but inverted, corrugation of the first substrate (Cu) layers exists.[28] The buckling of the Pb layer is considered to be the driving force for the "repulsion" of the bands at the crossing points and a gap opening. It has been suggested that this could provide a way for the adlayer to gain electronic energy, compensating the enhanced elastic energy of the reconstruction.[29] Comparing our data with these results, we could speculate that the band gap observed in Mn/Cu(110) alloy might be a consequence of the large buckling of the Mn and Cu layers as observed from the structural studies.[11] This is the first observation of such a band-gap opening observed in Mn-Cu alloys.

Figure 4(a) shows the Mn $2p$ core-level spectra for Mn deposition ranging from 0.125 to 5 ML. All spectra are characterized by two main peaks appearing at ~641.6 eV and ~651.6 eV binding energies corresponding to the spin-orbit split Mn $2p_{3/2}$ and $2p_{1/2}$ states, along with two pronounced shoulders, satellite peaks, appearing at higher binding energies. The intensity of these satellite features is almost equal up to 0.5 ML beyond which it drops systematically and practically vanishes for 5 ML coverage with the spectra resembling that of bulk Mn. These satellite features are manifestations of enhanced electron correlations in Mn/Cu(110) and were found also in Mn/Cu(100) (Ref. 10) and Mn/Ni(110).[12] The reduced Mn-Mn coordination in the $c(2\times2)$ structure, where ideally no Mn-Mn next-neighbor pairs exist, reduces considerably the overlap of the Mn $3d$-derived wave functions and thus the $3d$ bandwidth W. Also, in contrast to an fcc bulk site with 12 next-nearest neighbors, the Mn in the surface alloy has only eight neighbors placed further apart. Consequently, the electronic screening is reduced, resulting in the increase in the Coulomb correlation energy U and the U/W ratio. Beyond 0.5 ML, each Mn atom starts seeing other Mn atoms in its neighborhood. This results in the increase in Mn $3d$-$3d$ interactions, decrease in correlations, and hence reduced intensity of the satellite features. It was reported earlier that the satellite features disappear already for 1 ML in Mn/Cu(100) (Ref. 30) and 1.1 ML in Mn/Ni(110),[12] suggesting that the alloy ordering vanishes beyond those values (1–1.1 ML). In our case, the persistence of the satellite features even for 2.5 ML Mn goes along with the idea that the alloy order is maintained up to this high coverage. Furthermore, almost equal intensities of the satellite features for 0.125–0.5 ML suggest that the ordering of Mn atoms into the $c(2\times2)$ structure starts even for small Mn depositions, in agreement with the band-structure data of Fig. 3.

We notice further that the average satellite-to-main peak energy separations for $2p_{1/2}$ and $2p_{3/2}$ states are 5 eV and 3.5 eV, respectively, similar to what was found on Mn/Ag(001) (Ref. 31) and Mn/Cu(001).[30] Krüger and Kotani[32] demonstrated that the satellite structure is due to the presence of $2p^5 3d^5$ and $2p^5 3d^6 L^{-1}$ final states (where the ligand hole L^{-1} is mainly in the majority-spin Mn band of the neighboring atoms) and that atomic multiplet effects cause an apparent spin-orbit splitting that is greater for $3d^5$ than for $3d^6$ final states, leading to ~1 eV larger main line splitting for the $2p_{1/2}$ than for the $2p_{3/2}$ lines. Similar analysis for Mn/Cu(001) estimates an energy splitting of 3.5 eV and 5 eV for $2p_{3/2}$ and $2p_{1/2}$ components, respectively.[28] This exactly re-

produces our values for Mn/Cu(110). We may therefore conclude that the Mn $2p$ main peak is assigned to the well-screened state described as $2p^5 3d^6 L^{-1}$ and the satellite structure to the poorly screened state of $2p^5 3d^5$, where L^{-1} denotes the ligand hole on the neighboring Cu $3d$ and Mn $3d$ sites.

The Mn $L_{2,3}$ edge XAS spectra for various Mn concentrations are shown in Fig. 4(b). Besides the two pronounced edges corresponding to the spin-orbit split components L_3 and L_2, for Mn coverages $\leq$2.5 ML additional fine structures are observed: two shoulders at ~1 eV and ~3 eV higher energy of the L_3 peak and a doublet peak structure of the L_2 component. These well-resolved multiplet structures are again signatures of a localized ground state. The line shape of the present spectra coincides well with that reported for 0.2 ML Mn/Cu(110) previously.[33] The satellite features vanish at 5 ML, as in the case of the core-level photoemission spectra in Fig. 4(a), suggesting a crossover from a localized to an itinerant $3d$ electron behavior with increasing Mn coordination. Thus the Mn $2p$ absorption spectra reproduce our inferences from the core-level photoemission spectra confirming the role of electron correlations in dictating the electronic structure of this surface alloy.

Configuration-interaction cluster calculations of Mn $2p$ core-level spectra of analogous surface alloys $c(2\times2)$ Mn/Ni(110) and $c(2\times2)$ Mn/Cu(100) gives the parameters $\Delta=1.0$ eV, $U=3.0$ eV, and $dd\sigma=1.2$ eV (Ref. 12) for the former and $\Delta=1.5$ eV, $U=3.0$ eV, and $dd\sigma=1.0$ eV (Ref. 12) for the later, respectively, where Δ is the Ni (Cu) $3d$ to Mn $3d$ charge-transfer energy, U is the multiplet-averaged Mn $3d$-$3d$ interaction energy, and $dd\sigma$ is the Slater-Koster parameter expressing the hopping matrix elements between Mn $3d$ and Ni (Cu) $3d$ orbitals. Comparison of the above-mentioned two systems suggests that Δ and $dd\sigma$, but not U, vary slightly with the chemical environment (Ni and Cu, respectively). Keeping in mind that the structural relaxations for $c(2\times2)$ Mn/Cu(100) and $c(2\times2)$ Mn/Ni(100) have been found to be very similar to each other, a Mn relaxation of $0.06a$, where a is the lattice constant of Cu(110), as obtained from the structural analysis of Mn/Cu(110) has been used in the above-mentioned calculations for Mn/Ni(110). This suggests that the above approach is valid for our present case of Mn/Cu(110) also and will yield similar results. $\Delta<U$ suggests that in the Mn $2p$ XPS spectra, the main peak at lower binding energy is rather dominated by $2p^5 3d^6 L^{-1}$ and the satellite at higher binding energy by $2p^5 3d^5$ configurations as we have discussed previously. $\Delta\ll U$ also suggests that these surface alloys, $c(2\times2)$ Mn/Cu(110), $c(2\times2)$ Mn/Cu(100), $c(2\times2)$ Mn/Ni(110), etc., can be characterized as charge-transfer compounds, where in practice metallic conductivity of the systems will be provided by the Cu/Ni substrates.[12,34]

IV. CONCLUSIONS

To conclude, we investigated the evolution of the electronic structure and correlation effects in the Mn/Cu(110) surface alloy with increasing Mn concentration. We found that the Shockley surface state of Cu(110) gets strongly modified with Mn deposition, shifting systematically to higher binding energies with increasing Mn. The increase in the diameter of the surface-state Fermi contour suggests that Mn induces Cu charge reorganization and charge transfer into the surface state. This is accompanied by the appearance of new electronic bands at $\bar{X}$ that expose a gap of ~100 meV in the occupied states. The persistence of the correlation satellites in the Mn $2p$ core-level photoemission and absorption spectra over a wide range of Mn concentrations suggests an increased ordering of this alloy with respect to its counterparts on Cu(100) or Ni(110).

*unnikrishnan@tasc.infm.it

[1] B. Lu, X. Liu, K. Nakatsuji, T. Iimori, and F. Komori, Phys. Rev. B **76**, 245433 (2007).
[2] Y. Huttel, C. M. Teodorescu, F. Bertran, and G. Krill, Phys. Rev. B **64**, 094405 (2001).
[3] M. Wuttig, Y. Gauthier, and S. Blügel, Phys. Rev. Lett. **70**, 3619 (1993).
[4] M. Eder, J. Hafner, and E. G. Moroni, Phys. Rev. B **61**, 11492 (2000).
[5] O. Rader, W. Gudat, C. Carbone, E. Vescovo, S. Blügel, R. Kläsges, W. Eberhardt, M. Wuttig, J. Redinger, and F. J. Himpsel, Phys. Rev. B **55**, 5404 (1997).
[6] W. L. O'Brien and B. P. Tonner, Phys. Rev. B **51**, 617 (1995).
[7] M. Wuttig, S. Junghans, T. Flores, and S. Blügel, Phys. Rev. B **53**, 7551 (1996).
[8] C. L. Fu, A. J. Freeman, and T. Oguchi, Phys. Rev. Lett. **54**, 2700 (1985).
[9] S. Blügel, Phys. Rev. Lett. **68**, 851 (1992).
[10] O. Rader, E. Vescovo, M. Wuttig, D. D. Sarma, S. Blügel, F. J. Himpsel, A. Kimura, K. S. An, T. Mizokawa, A. Fujimori, and C. Carbone, Europhys. Lett. **39**, 429 (1997).
[11] Ch. Ross, B. Schirmer, M. Wuttig, Y. Gauthier, G. Bihlmayer, and S. Blügel, Phys. Rev. B **57**, 2607 (1998).
[12] O. Rader, T. Mizokawa, A. Fujimori, and A. Kimura, Phys. Rev. B **64**, 165414 (2001).
[13] G. Panaccione, I. Vobornik, J. Fujii, D. Krizmancic, E. Annese, L. Giovanelli, F. Maccherozzi, F. Salvador, A. De Luisa, D. Benedetti, A. Gruden, P. Bertoch, F. Polack, D. Cocco, G. Sostero, B. Diviacco, M. Hochstrasser, U. Maier, D. Pescia, C. H. Back, T. Greber, J. Osterwalder, M. Galaktionov, M. Sancrotti, and G. Rossi, Rev. Sci. Instrum. **80**, 043105 (2009).
[14] K. Berge, A. Gerlach, G. Meister, A. Goldmann, and E. Bertel, Phys. Rev. B **70**, 155303 (2004).
[15] T. Andreev, I. Barke, and H. Hövel, Phys. Rev. B **70**, 205426 (2004).
[16] F. Forster, S. Hüfner, and F. Reinert, J. Phys. Chem. B **108**, 14692 (2004).
[17] A. Tamai, A. P. Seitsonen, F. Baumberger, M. Hengsberger, Z.-X. Shen, T. Greber, and J. Osterwalder, Phys. Rev. B **77**, 075134 (2008).

[18] A. Ferretti, C. Baldacchini, A. Calzolari, R. Di Felice, A. Ruini, E. Molinari, and M. G. Betti, Phys. Rev. Lett. **99**, 046802 (2007).
[19] K. Kanazawa, Y. Sainoo, Y. Konishi, S. Yoshida, A. Taninaka, A. Okada, M. Berthe, N. Kobayashi, O. Takeuchi, and H. Shigekawa, J. Am. Chem. Soc. **129**, 740 (2007).
[20] S. A. Lindgren and L. Walldén, Solid State Commun. **28**, 283 (1978).
[21] E. Bertel, Surf. Sci. **331-333**, 1136 (1995).
[22] M. Preuss, W. G. Schmidt, and F. Bechstedt, Phys. Rev. Lett. **94**, 236102 (2005).
[23] W. G. Schmidt, K. Seino, M. Preuss, A. Hermann, F. Ortmann, and F. Bechstedt, Appl. Phys. A: Mater. Sci. Process. **85**, 387 (2006).
[24] I. Vobornik, J. Fujii, M. Mulazzi, G. Panaccione, M. Hochstrasser, and G. Rossi, Phys. Rev. B **72**, 165424 (2005).
[25] I. Vobornik, J. Fujii, M. Hochstrasser, D. Krizmancic, C. E. Viol, G. Panaccione, S. Fabris, S. Baroni, and G. Rossi, Phys. Rev. Lett. **99**, 166403 (2007).
[26] M. Mulazzi, G. Rossi, J. Braun, J. Minàr, H. Ebert, G. Panaccione, I. Vobornik, and J. Fujii, Phys. Rev. B **79**, 165421 (2009).
[27] F. Schiller, S. V. Halilov, and C. Laubschat, Phys. Rev. B **65**, 184430 (2002).
[28] S. Müller, J. E. Prieto, C. Rath, L. Hammer, R. Miranda, and K. Heinz, J. Phys.: Condens. Matter **13**, 1793 (2001).
[29] F. Baumberger, A. Tamai, M. Muntwiler, T. Greber, and J. Osterwalder, Surf. Sci. **532-535**, 82 (2003).
[30] A. Kimura, S. Asanao, T. Kambe, T. Xie, S. Watanabe, M. Taniguchi, S. Qiao, E. Hashimoto, H. Namatame, T. Muro, S. Imada, and S. Suga, Phys. Rev. B **76**, 115416 (2007).
[31] P. Schieffer, C. Krembel, M. C. Hanf, and G. Gewinner, J. Electron Spectrosc. Relat. Phenom. **104**, 127 (1999).
[32] P. Krüger and A. Kotani, Phys. Rev. B **68**, 035407 (2003).
[33] H. A. Dürr, G. van der Laan, D. Spanke, F. U. Hillebrecht, and N. B. Brookes, Phys. Rev. B **56**, 8156 (1997).
[34] U. Manju, V. P. S. Awana, H. Kishan, and D. D. Sarma, Phys. Rev. B **74**, 245106 (2006); D. D. Sarma, J. Solid State Chem. **88**, 45 (1990); S. Nimkar, D. D. Sarma, and H. R. Krishnamurthy, Phys. Rev. B **47**, 10927(R) (1993).